EBioMedicine 40 (2019) 663–674

Contents lists available at ScienceDirect

EBioMedicine

journal homepage: www.ebiomedicine.com

EBioMedicine
Published by THE LANCET

Salt-deficient diet exacerbates cystogenesis in ARPKD via epithelial sodium channel (ENaC)

Daria V. Ilatovskaya [a,1], Vladislav Levchenko [a], Tengis S. Pavlov [a,2], Elena Isaeva [a], Christine A. Klemens [a], Jessica Johnson [a], Pengyuan Liu [a], Alison J. Kriegel [a], Alexander Staruschenko [a,b,*]

[a] Department of Physiology, Medical College of Wisconsin, 8701 Watertown Plank Road, Milwaukee, WI 53226, USA
[b] Clement J. Zablocki VA Medical Center, 5000 West National Avenue, Milwaukee, WI, 53295, USA

ARTICLE INFO

Article history:
Received 14 November 2018
Received in revised form 4 January 2019
Accepted 5 January 2019
Available online 8 February 2019

Keywords:
Autosomal Recessive Polycystic Kidney Disease (ARPKD)
Cysts development
Epithelial Sodium Channel (ENaC)
miR-9a
Salt diets
Renin-angiotensin-aldosterone system (RAAS)

ABSTRACT

Background: Autosomal Recessive Polycystic Kidney Disease (ARPKD) is marked by cyst formation in the renal tubules, primarily in the collecting duct (CD) system, ultimately leading to end-stage renal disease. Patients with PKD are generally advised to restrict their dietary sodium intake. This study was aimed at testing the outcomes of dietary salt manipulation in ARPKD.
Methods: PCK/CrljCrlPkhd1pck/CRL (PCK) rats, a model of ARPKD, were fed a normal (0.4% NaCl; NS), high salt (4% NaCl; HS), and sodium-deficient (0.01% NaCl; SD) diets for 8 weeks. Immunohistochemistry, GFR measurements, balance studies, and molecular biology approaches were applied to evaluate the outcomes of the protocol. Renin-angiotensin-aldosterone system (RAAS) levels were assessed using LC-MS/MS, and renal miRNA profiles were studied.
Findings: Both HS and SD diets resulted in an increase in cystogenesis. However, SD diet caused extensive growth of cysts in the renal cortical area, and hypertrophy of the tissue; RAAS components were enhanced in the SD group. We observed a reduction in epithelial Na^+ channel (ENaC) expression in the SD group, accompanied with mRNA level increase. miRNA assay revealed that renal miR-9a-5p level was augmented in the SD group; we showed that this miRNA decreases ENaC channel number in CD cells.
Interpretation: Our data demonstrate a mechanism of ARPKD progression during salt restriction that involves activity of ENaC. We further show that miR-9a-5p potentially implicated in this mechanism and that miR-9a-5p downregulates ENaC in cultured CD cells. Our findings open new therapeutic possibilities and highlight the importance of understanding salt reabsorption in ARPKD.

1. Introduction

Autosomal Recessive Polycystic Kidney Disease (ARPKD) is a genetic disorder that results in progressive cyst formation in the renal tubules, including the collecting duct (CD) system [1], ultimately leading to renal insufficiency and end-stage renal disease. ARPKD is primarily a childhood nephropathy, occurring 1 in 20,000 of live births. Up to 30% of ARPKD patients die during the neonatal period. Major clinical phenotypes that manifest in the kidney are dilatation of the CDs and systemic hypertension; the vast majority of survivors have renal insufficiency, and up to a third undergo kidney transplantation [2,3]. Despite the fact that a mutant gene responsible for the disease, *PKDH1*, has been identified and there are orthologous animal models available, the pathogenesis of the disease remains essentially unknown. The cellular defects that might be responsible for the clinical manifestations of ARPKD are understudied, and no effective therapies exist to date.

Patients with chronic kidney disease (CKD) are at risk of exhibiting increased extracellular volume, and therefore low-sodium diets are often prescribed to limit complications in this condition [4–6]. Many recent studies suggest that a low sodium diet may not be as beneficial for all CKD patients as was previously thought. The Center for Nutrition Policy and Promotion recommends a daily sodium intake of <2300 mg in the general population and 1500 mg for high-risk patients [7]. Unfortunately, the extent to which dietary sodium restriction benefits patients is not fully understood, especially taking into consideration the various causes leading to CKD [6]. A comprehensive review on salt and health and current experience of worldwide salt reduction programs [5] indicated that modest reduction in population salt intake should result in a major improvement in public health. However, more recent data

* Corresponding author at: Department of Physiology, Medical College of Wisconsin, 8701 Watertown Plank Road, Milwaukee, WI 53226, USA.
E-mail address: staruschenko@mcw.edu (A. Staruschenko).
[1] Present address: Department of Medicine, Division of Nephrology, Medical University of South Carolina, Charleston USA.
[2] Present address: Division of Hypertension and Vascular Research, Henry Ford Hospital, Detroit USA .

https://doi.org/10.1016/j.ebiom.2019.01.006

Research in context

Evidence before this study

Autosomal Recessive Polycystic Kidney Disease (ARPKD) is an inherited nephropathy marked by cyst formation in the renal tubules, primarily in the collecting duct (CD) system, eventually leading to renal insufficiency. Up to 30% of ARPKD patients die during the neonatal period, and up to a third of survivors have to undergo kidney transplantation. Despite the severity of the disease, our knowledge about the ion transport properties of the cells comprising the cysts in ARPKD remains limited. Generally, patients with ARPKD are advised to limit their sodium intake, as it is expected to reduce blood pressure and albuminuria. However, the long-term effects of salt restriction have not been studied in ARPKD.

Added value of this study

Here we aimed to study the outcomes of different dietary sodium consumption in an animal model of ARPKD to investigate the mechanisms involved in salt-level mediated cystogenesis. In PKD patients' management, the diet and food behavior are important factors of therapy because this provides an affordable and safe way to limit progression of the disease. Although a low salt diet is considered beneficial for individuals suffering from chronic kidney disease, there has been no comprehensive research with regards to specific dietary sodium content that should be recommended to ARPKD subjects. Several recent research studies actually targeted renal sodium transport in autosomal dominant PKD, although the results are conflicting, and the mechanisms which link sodium transport and cystogenesis remain to be elucidated. This study uncovers a novel aspect of ARPKD.

Implications of all the available evidence

First and foremost, we demonstrate a dramatic exacerbation of cortical cyst formation and rapid progression to kidney failure in salt-restricted ARPKD rats. Then, we show evidence that Epithelial Na^+ Channel (ENaC), expressed in the CDs, is downregulated during this salt-restriction, and there are a number of miRNAs that are differentially expressed depending on dietary sodium content. In cell culture studies we revealed that among these miRs, miR-9a-5p is able to downregulate ENaC. Our findings open new avenues of research and potential caution that needs to be exercised regarding dietary sodium in order to enhance our understanding of the control of salt balance and cystogenesis in ARPKD.

pointed out that there is a need for studies specifically designed to assess salt intake as an endpoint in order to evaluate the mechanisms and safety of reduced salt intake [8]. Current findings suggest that there is a U-shaped rather than a linear relationship between sodium intake and cardiovascular outcomes [6]. Of interest is the finding that in patients without renal disease both higher sodium excretion and lower sodium excretion are associated with an increase in cardiovascular death [9]. At this point there is no clear consensus on whether low sodium intake is beneficial or harmful. Attention to patients' diet is especially important because PKD treatment involves years of consuming of various drugs which have potentially adverse effects. For example, dietary caloric restriction is recognized a perspective strategy reducing Warburg effect typical for polycystic kidneys effective in the experimental settings [10].

In 2015 the Kidney Disease: Improving Global Outcomes (KDIGO) Controversies Conference published a summary statement for PKD, stating that their "diagnosis, evaluation, prevention, and treatment vary widely and there are no broadly accepted practice guidelines" [11]. Currently tolvaptan is approved to treat ADPKD (autosomal dominant PKD) in Europe, Canada, Japan, and USA. Unfortunately, there is no treatment for ARPKD available to date. Generally, PKD patients are advised to restrict their dietary sodium intake, as this is expected to reduce blood pressure and albuminuria [12–17]. Although a low salt diet is usually considered beneficial for individuals with CKD [4–6], there has been no comprehensive research pertaining to dietary sodium content recommended for ARPKD subjects. PKD patients report receiving conflicting advice from their physicians with regards to sodium levels in their food [12]. Several recent research studies actually targeted renal sodium transport in ARPKD or ADPKD [16–18], but the mechanisms linking sodium transport and cystogenesis require further investigation.

There has been more comprehensive research done on sodium intake in the area of ADPKD compared to ARPKD. In a recent post hoc analysis of the HALT-PKD clinical trial, dietary sodium restriction was retrospectively shown to be beneficial to the management of ADPKD [16]. Ongoing research is determining why high sodium intake is associated with larger kidneys and a faster decline in renal function in ADPKD [5,16]. In 2017, a pilot ADPKD intervention study by Taylor et al. demonstrated that there is a solid basis to justify a clinical trial featuring administration of experimental low sodium diets to ADPKD patients, with the ultimate goal of ameliorating hypertension, renal pain, and the progression of renal dysfunction [17]. In CDs, the rate limiting step for Na^+ reabsorption is epithelial sodium channel (ENaC) activity [19], which is a compelling target for ARPKD. A recent study by Germino's group [20] demonstrated that ENaC expression and activity (amiloride-sensitive current recorded in primary cystic monolayers) are increased in ARPKD. Earlier studies by others also suggested that hypertension in ARPKD could be due in part to enhanced sodium reabsorption in the CD and increased ENaC activity [21,22]. Our data demonstrated that renal ENaC activity is lower in the freshly isolated ARPKD epithelia, however, cyst formation is exacerbated upon administration of an ENaC inhibitor amiloride [23]. In this study using a PCK (PCK/CrljCrl-Pkhd1pck/CRL) rat as an ARPKD model, we tested the effects of low and high sodium intake on cystogenesis in ARPKD, and explored possible molecular mediators of these effects, including changes in ENaC in the cysts.

2. Materials and methods

2.1. Experimental protocol

Here we used an established animal model of ARPKD – the PCK/CrljCrlPkhd1pck/CRL (PCK) rat initially kept on a standard Purina 5001 diet. This strain was derived from a Sprague Dawley (SD) outbreeding colony [24] and is a spontaneous hereditary model; the responsible gene, *Pkhd1*, is located on rat chromosome 9 and is orthologous to the gene affected in human ARPKD. Initial renal cysts in these rats originate from the CDs, and at the later stages of the disease cysts diffusely affect whole nephron segments; hepatic and pancreatic cysts are also observed similar to humans [25,26]. Routine metabolic cage studies and GFR measurements were employed to assess renal function in PCK rats fed a normal (0.4% NaCl, NS), high salt (4% NaCl, HS), and sodium-deficient (0.01% NaCl, SD) diets based on purified AIN-76A rodent food (Dyets, Inc., #D113755, Bethlehem, PA) for 8 weeks starting at 6 weeks of age. At the end of the protocol, tissues were collected after kidney flush as done previously [27]. PCK rats were obtained from Charles River Laboratories Inc. Animal use and welfare adhered to the NIH Guide for the Care and Use of Laboratory Animals following a protocol reviewed and approved by the IACUC of the Medical College of Wisconsin.

2.2. Biochemical measurements

Urine measurements were taken in metabolic cages (40,615; Laboratory Products) throughout the protocol during the dietary salt treatment; Na^+, K^+, Cl^-, and Ca^{2+} levels, as well as urinary creatinine were measured with a blood gas analyzer ABL800 FLEX (Radiometer America Inc.); blood electrolyte levels were analyzed in freshly collected samples using the same instrument. Copeptin and aldosterone urinary levels were measured with ELISA kits according to the manufacturer's guide (LSBio LifeSpan BioSciences Inc. (LS-F9056) and Enzo Lifesciences (ADI-900-173), respectively). To characterize circulating RAS levels, we employed the services of Attoquant Diagnostics LLC (Austria); they use ultra-pressure-liquid chromatography-tandem mass spectrometry (LC-MS/MS) and stable-isotope-labeled internal standards that provide superior specificity and sensitivity compared to antibody testing.

2.3. Histochemistry and analysis of cystic index

Isolated kidneys and livers were fixed in 10% formalin and routinely embedded, cut at 4 μm slices, dried and deparaffinized for subsequent histochemical analysis. H&E (haemotoxylin and eosin) staining was used to assess organ morphology. Then, organ slices were scanned with Nikon Super CoolScan 8000 and further analyzed using ImageJ (https://imagej.nih.gov/ij/) to examine the cyst prevalence in relation to the total area of the organ slice. The analysis was performed by first converting images to 8 bit, selecting whole kidney slice as a region of interest (ROI), and then thresholding the image in order to discern cystic areas from tissue. Analyze Particles plugin in ImageJ software was then utilized to calculate the percent of the thresholded area in the ROI.

2.4. Measurement of GFR in conscious rats

GFR was measured in unrestrained conscious rats using a high-throughput method featuring detection of fluorescent FITC-labeled inulin (TdB Consultancy AB, Uppsala, Sweden) clearance from blood. The method was adapted for rats from a protocol previously described for mice by Rieg [28] and also published by us earlier [29]. Pre-dialyzed 20 mg/mL of FITC-inulin solution in saline (2 μL of 2% solution per 1 g of body weight) was administered by a bolus tail vein injection to rats briefly anesthetized with isoflurane. Immediately after the injection anesthesia was discontinued, and the animals were allowed to regain consciousness. Then, 10 μL of blood was collected 3, 5, 8, 16, 25, 40, 60, 80, 100, and 120 min after the injection by tail bleed. Next, plasma was separated, and inulin clearance was quantified by FITC intensity. Fluorescence measurements were performed using a NanoDrop 3300 Fluorospectrometer (Thermo Fisher Scientific, Wilmington, DE, USA). GFR was then calculated from the observed decrease in FITC fluorescence using a two-compartment model (the initial fast decay representing the redistribution of FITC-inulin from the intravascular compartment to the extracellular fluid, and the slower phase reflecting clearance from plasma). The GFR curves were approximated with a bi-exponential decay function using OriginPro 9.0 (OriginLab, Northhampton, MA) software, and GFR values in mL/min were obtained from the fitting parameters using the previously described equation [28].

2.5. mCCD cell culture and transfection

Mouse cortical collecting duct (mCCDcl-1) cells provided by Dr. Rossier were cultured in 75-cm flasks for up to 10 passages in Dulbecco's Minimum Essentials Medium (DMEM) supplemented with 2% Fetal Bovine Serum (FBS), 5 μg/mL insulin, 5 μg/mL human apo-Transferrin, 10 ng/mL epidermal growth factor (EGF), 1 nM triiodo-L-thyronine sodium salt, 60 nM sodium selenite, 50 nM dexamethasone, 100 units/mL penicillum, 100 μg/mL streptomycin, and 100 μg/mL Normocin™ (Invitrogen, San Diego, CA), as previously described [31]. The day before transfection, cells were seeded into 35 mm cell culture dishes. Cells were transiently transfected at 50% confluency with 25 nM mirVana negative control miRNA mimic or 25 nM hsa-miR-9-5p mirVana miRNA mimic (ThermoFisher) using Lipofectamine 2000 (ThermoFisher) according to manufacturer's instructions. Transfected or naïve cells were used for electrophysiological and Western blot experiments 24 h after transfection.

2.6. Measurement of ENaC single-channel activity in the cell-attached mode

The mCCDcl-1 cells mounted on glass chips were transferred from the incubator to a recording chamber containing extracellular solution (in mM): 145 NaCl, 4.5 KCl, 1 $CaCl_2$, 2 $MgCl_2$, and 10 HEPES (pH 7.35) and allowed to rest for at least 10 min prior to recording. All experiments were carried out at room temperature (21–23 °C). Patch electrodes were made from borosilicate glass capillaries (1B150F-4, World Precision Instruments) and had a resistance of 6–10 MΩ when filled with a solution of the following composition (in mM): 140 LiCl, 2 $MgCl_2$, and 10 HEPES (pH 7.35). Single-channel activity recordings were made using an Axopatch200B amplifier (Molecular Devices, Sunnyvale, CA, USA), low-passed at 0.1 kHz by an eight-pole Bessel filter (Warner Instruments, Hamden, CT, USA), digitized at 1 kHz using a Digidata 1440A acquisition board (Molecular Devices) and stored in the PC hard drive. After the formation of gigaseal contact, ENaC activity was monitored at a membrane voltage of −60 mV for several minutes. For the current-voltage relationship, ENaC current was recorded at applied membrane voltages from −80 to 0 mV with 20 mV steps. Data were acquired using pClamp 10.6 software and analyzed as previously reported [30].

2.7. Western blotting

Kidney cortical lysates were prepared as follows. Animal kidneys were flushed with PBS in an anesthetized animal, excised and cut in 1- to 2-mm slices under a dissection scope. Approximate cortical sections were carved, weighted and dissolved in Laemmli with a protease and phosphatase inhibitors (Roche) at 20 mg/ml with pulse sonication for 5–10 s. Samples were subjected to PAGE, transferred onto nitrocellulose membrane (Millipore) for antibody hybridization, and subsequently visualized by enhanced chemiluminescence (ECL; Amersham Biosciences). For Western blots from mCCD cells, equal numbers of cells were lysed in Laemli buffer with protease inhibitors (Roche) and pulse sonicated before being run as described above for the kidney lysates. Antibodies: α-ENaC (ext) – Alomone Cat #: ASC-030; AQP-2 – SCBT Cat # sc-9882; β-Actin – SCBT Cat # sc-1616 HRP, α-, β-, γ-ENaC –Stressmarq Cat#: SPC-403, SPC-404, and SPC-405 respectively.

2.8. RNA isolation and PCR analysis

Total RNA from flash frozen thin cortical kidney sections was isolated using TRIzol Reagent (ThermoFisher) according to manufacturer's protocol. Total RNA quantity was determined by Nanodrop 2000 (ThermoFisher). RNA quality was verified using Agilent 2100 Bioanalyzer, and only samples with RNA integrity numbers (RIN) >8 were used. cDNA from 2 μg of RNA was generated using the RevertAid First Strand cDNA Synthesis Kit (ThermoFisher) with random hexamer primers. Real-time PCR reactions were carried out on an ABI Prism 7900HT (ABI, Applied Biosytems, Foster City, CA) using Bullseye EvaGreen qPCR Master Mix (MedSci, Valley Park, MO) according to manufacturer's directions in 10 μL final volume with samples run in triplicate. Final Ct values were determined using SDS software, version 2.3. Exon spanning primers were designed from the rat sequences of *Scnn1a*, *Scnn1b*, *Scnn1g* (sodium channel epithelial 1 alpha/beta/gamma subunits), *Aqp2* (aquaporin 2), and *18 s* (18S ribosomal RNA) (see Table 1) and assessed for specificity via sequencing of the PCR

Table 1
Exon spanning primers were designed from the rat sequences of Scnn1a, Scnn1b, Scnn1g, Aqp2, and 18s.

18S F	CGGCTACCACATCCAAGGAA
18S Rev	CCTGTATTGTTATTTTTCGTCACTACCT
Scnn1a F	CCCTGCAACCAGGCGAATTA
Scnn1a Rev	TCCTGACCATGCACCATCAC
Scnn1b F	GAGCTGCCTTCTTGGGTTCT
Scnn1b Rev	CCACACGATATTGTTGGCCG
Scnn1g F	TCACGCTTTTCCACCATCCA
Scnn1g Rev	GATGACTTGCAGCCCGTACT
Aqp2 F	GCCACCTCCTTGGGATCTATT
Aqp2 Rev	AAGACCCAGTGATCATCAAACTTG

product. Quantification of α-, β, and γ-ENaC subunit and AQP2 (aquaporin 2) mRNA copy number was determined by normalizing to 18S.

2.9. miRNA screening and related statistics

Total RNA was extracted using a Trizol-based method and quantified by Nanodrop [32]. Small RNA deep sequencing and analysis was performed as previously described by the Genomic Sciences and Precision Medicine Center (GSPMC) at the Medical College of Wisconsin [33]. Differential expression was determined by edgeR2 method [34]. False discovery rate within statistical analysis was controlled for using the Benjamini-Hochberg method. Targetscan (http://www.targetscan.org) was used to identify miRNA targets. A Taqman miRNA assay (ThermoFisher) for miR-9 was performed as previously described [32], with data normalized to expression of ribosomal 5s, to evaluate efficacy of miR-9-5p mimic transfection conditions to be used in subsequent experiments. Differentially expressed miRNAs were selected based on a cut off value for the fold increase or decrease (2-fold increase/decrease cut off was chosen) and adjusted p-value of <0.05). Raw data are deposited in GEO.

2.10. Statistics

All summarized data are reported as mean ± SEM. Data reported as box plots reports all data points, with the box showing SEM and error bars showing SD. Data is compared using the one-way analysis of variance (ANOVA) followed by a Bonferroni, Holm-Sidak or Tukey post-hoc tests, or with Mann-Whitney Rank Sum test. Differences were considered statistically significant at $P < .05$. GFR curves for FITC-inulin clearance were fitted with a nonlinear curve fit (ExpDec2) function using OriginPro 9.0 with a Levenberg Marquardt iteration algorithm with 5 degrees of freedom, adjusted R-squared >0. For miRNA Western blots, following a Shapiro-Wilk normality test, control and experimental values were compared using an unpaired student t-test.

3. Results

3.1. Experimental design and physiological parameters measured in PCK rats throughout the protocol

Three groups of PCK rats were switched to normal (0.4% NaCl, NS), high salt (4% NaCl, HS), or sodium-deficient (0.01% NaCl, SD) diets at 6 weeks of age (see Fig. 1A for the schematic representation of the experimental protocol; initially animals were fed standard Purina 5001 diet). During an 8-week dietary treatment routine metabolic cage studies were performed. Daily diuresis assessment revealed a dramatic increase in urinary output in the group fed a HS diet, and a lesser but still a significant increase in the SD diet fed animals, both in comparison to a NS diet fed group (Fig. 1B). Food intake remained similar among all three groups of animals (Fig. 1C), whereas animal growth (as represented by body weight) was found to be significantly attenuated in the group fed a SD diet (Fig. 1D). Urinary electrolyte levels measured throughout the experimental protocol are shown in Supplementary Fig. S1B; urinary potassium (normalized to creatinine) did not differ between the groups, and indirectly supports food intake data since potassium content was the same in all tested diets. At the end of the experiment, kidneys were cleared from blood with a flush via the abdominal aorta, collected and weighed. As seen on Fig. 1E, we observed an increase in kidney weight (as well as tissue hypertrophy, also seen in Fig. 3A) in the group fed a SD diet. Additionally, plasma electrolyte levels measured at the end of the experiment (Supplementary Fig. S1A) revealed a dramatic drop in plasma levels of sodium, chloride, potassium and calcium in SD diet fed animals compared to both NS and HS diet fed experimental groups.

3.2. Renal function is impaired in the PCK rats fed a salt-deficient diet

Using high-throughput and minimally invasive glomerular filtration rate (GFR) measurements in conscious freely moving rats (adapted from a mouse protocol [28]) – we were able to demonstrate a dramatic decline in GFR in the salt restricted animals, after 8 weeks of salt-deficient diet (Fig. 2A). GFR levels were found to be 0.40 ± 0.05, 0.65 ± 0.03, and 0.98 ± 0.11 mL/min/100 g of body weight in SD, NS and HS fed rats, respectively. Blood urea nitrogen (BUN), a marker of renal function decline, was tested in plasma of all experimental animals at the end of the protocol, and it was found to be almost 10 times higher in the SD compared to NS and HS diet fed groups (129.6 ± 9.8, 17.3 ± 0.9, and 14.2 ± 0.9 mg/dL in SD, NS and HS fed rat plasma, respectively, Fig. 2B).

3.3. Renal and hepatic cyst development in the PCK rats fed diets with varying salt content

Next, we performed histological examination of renal and hepatic tissues from the studied groups to assess cystic index. As seen in Fig. 3, cystic area was elevated both in liver and in kidney when animals were fed a SD diet, although in renal tissue the effect of salt restriction on cystogenesis was more pronounced. We observed more than a 20% increase in renal cyst formation in the group of PCK rats fed a 0.01% NaCl; of interest is the finding that salt restriction promoted major cyst formation specifically in the cortical area of the kidney, which was not observed at such high rates in NS and HS fed animals. Cysts area in cortex on NS or HS diets were 14.1 ± 2.2% or 17.5 ± 1.1%, respectively, whereas SD diet caused massive development of cortical cysts up to 33.8 ± 3.8% (Fig. 3B). Similar to the kidney, cystic area in liver from SD treated PCK rats was significantly elevated (Figs. 3C and D).

3.4. Vasopressin and renin-angiotensin-aldosterone system (RAAS) signaling in the PCK rats upon sodium restriction and salt challenge

The following experiments were designed to test potential mechanisms contributing to cyst development in the dietary groups. First, we evaluated vasopressin signaling by measuring urinary copeptin levels as a vasopressin surrogate marker (ELISA); copeptin was undetectable in the urine of the HS diet fed PCK rats, and was found to be slightly (although not statistically significantly) elevated in SD group compared to NS animals (Fig. 4A). We next performed a comprehensive biochemical characterization of the soluble Renin-Angiotensin System (RAS) in the rats' plasma using "RAS (renin-angiotensin-system) Fingerprint" analysis by Attoquant Diagnostics GmbH (Austria). Our results indicated that all components of circulating RAS were significantly enhanced in animals fed a salt-deficient diet (Ang (angiotensin) I, Ang II, Ang III, Ang IV, Ang 1-5, Ang 1-7; Fig. 4B shows Angiotensin II level; please refer to Fig. S2 for the full panel featuring Ang I, Ang III, Ang IV, Ang 1-7, Ang 1-5, ACE (angiotensin-converting-enzyme) activity and prorenin receptor activity (PRA)). We also tested aldosterone levels both in plasma and urine of the experimental animals. Our results depicted in Fig. 4C revealed significantly augmented circulating and urinary aldosterone levels in rats fed a SD diet compared to NS and HS diet fed groups, aligning with our data demonstrating elevation of other RAS components. Interestingly, plasma potassium level measurements

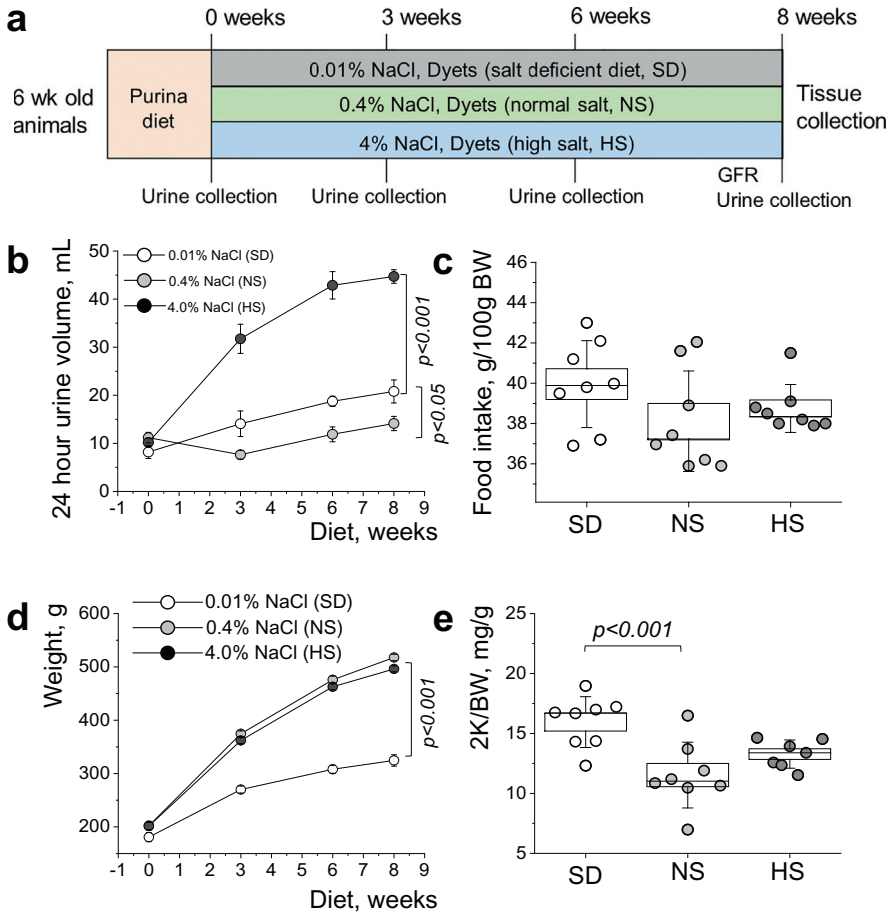

Fig. 1. Study protocol and basic physiological parameters assessment throughout the study. (a) Experimental protocol showing the 3 groups of PCK rats studied on normal (0.4% NaCl, NS), high salt (4% NaCl, HS), and sodium-deficient (0.01% NaCl, SD) diets for 8 weeks starting at 6 weeks of age. Metabolic cage urine collections and GFR measurements were performed throughout the protocol. Values were compared using a repeated-measures ANOVA. (b,c) Daily urinary output (b) and food intake (c) of the experimental groups measured during the study. (d,e) Body weight (d) and two kidneys to body weight ratio (2 K/BW, (e)) data was obtained from the animals at the end of the experimental protocol. Values were compared using a repeated-measures ANOVA with Holm-Sidak post-hoc (d) and one-way ANOVA with a Tukey post-hoc test (e). In box plots, the box is SEM, whiskers represent SD, and the line within the box shows the median value. $N = 8$ animals per group.

(Supplementary Fig. S1) revealed a significant drop in plasma in the SD diet fed rats.

3.5. miR-9a-5p may affect Na^+ channel (ENaC) protein expression in the cortex of the PCK rats fed a salt-deficient diet

Since ENaC is the rate-limiting step for Na^+ reabsorption in the collecting duct and contributes to the cysts development in PCK rats, we tested ENaC protein and mRNA expression in the cortical renal tissue. As shown in Fig. 5A, there is a dramatic reduction in αENaC subunit expression in the group of PCK rats fed a SD diet, accompanied with a significant increase in corresponding mRNA as well as mRNA for β-, and γ-ENaC subunits (Fig. 5B). We next tested if AQP2 (aquaporin 2) levels are altered in animals after NS or HS dietary challenge, and observed a significant increase in AQP2 expression on both SD and HS diet challenges (Fig. 5C).

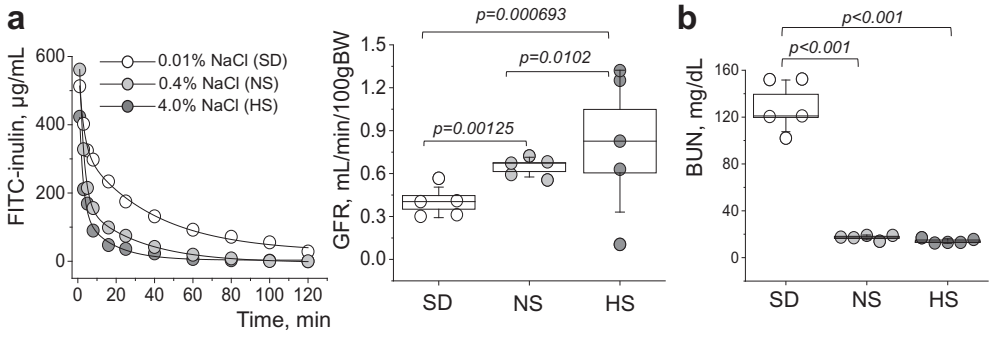

Fig. 2. Kidney injury in PCK rats fed diets with different sodium content. (a) Representative FITC-inulin clearance curves (left) and a summarizing graph showing GFR levels (right) obtained from PCK rats fed normal (0.4% NaCl, NS), high salt (4% NaCl, HS), and sodium-deficient (0.01% NaCl, SD) diets at the end of the experimental protocol. (b) Plasma BUN values in PCK rats fed a NS, HS and SD diets. $N = 8$ animals per group. Values were compared using a one-way ANOVA with a Tukey post-hoc test. In box plots, the box is SEM, the whiskers represent SD, and the line within the box shows median value.

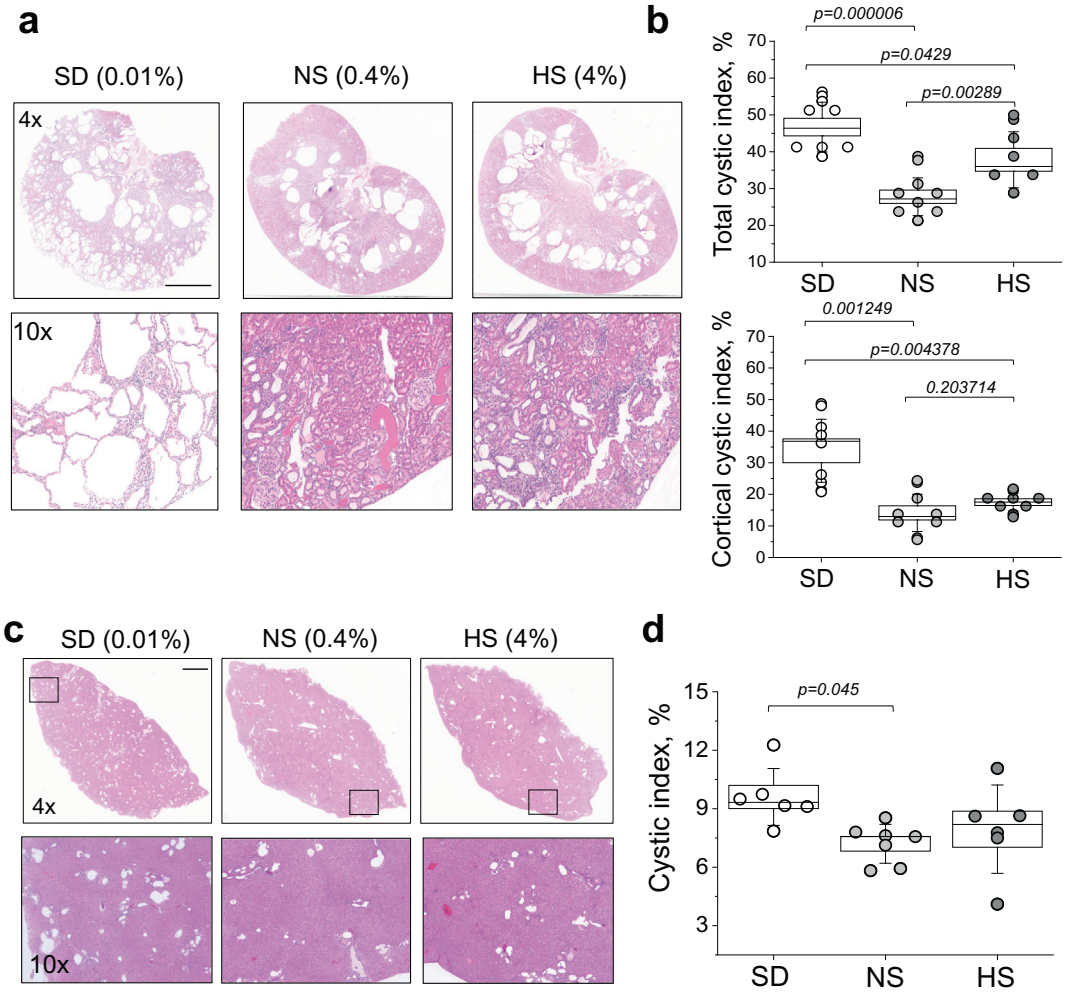

Fig. 3. Renal cyst development in PCK rats fed diets with different sodium content. (a) Upper panel shows representative images from H&*E*-stained kidney tissues of PCK rats fed a SD, NS and HS diets according to the experimental protocol. The scale bar (3 mm) is common for all top row images; the lower row of images demonstrates blown-up regions of cortical area from the upper images. (b) Summary graphs illustrating cystic index (percent of cysts relative to tissue slice area) in relation to whole kidney slices, and cystic index specifically in the cortical renal area of PCK rats fed a SD, NS and HS diets. Tissues from a minimum of 7 animals per group were analyzed. (c) Hepatic cyst development in PCK rats fed diets with different sodium content. Upper panel shows representative images from H&E-stained liver tissues of PCK rats fed a SD, NS and HS diets according to the experimental protocol. The scale bar shown is common for all top row images and is 2 mm; the lower row of images demonstrates liver regions expanded from the upper panel. (d) Summary graph illustrating cystic index (percent of cysts relative to tissue slice area) in the livers of PCK rats fed a SD, NS and HS diets. Tissues from at least 6 animals per group were analyzed. Values were compared using a one-way ANOVA with a Tukey post-hoc test. In box plots, the box is SEM, whiskers represent SD, and line within the box shows median value.

Taking into consideration the possibility that miRNA regulation could be responsible for the discrepancy between the αENaC protein expression and mRNA levels we detected, we performed small RNA sequencing on RNA isolated from cortical tissues of experimental animals. We did not find any miRNAs that were differentially expressed between the NS and HS diet fed groups; however, there were 7 miRs identified which were differentially expressed between SD and NS or SD and HS diet fed groups (cut off was based on 2-fold increase or decrease and adjusted *p*-value of <0.05). Among these miRs, shown in Fig. 5D, miR-9a-5p specifically was predicted to interact with the 3′ untranslated region (UTR) of the βENaC subunit (see Methods), and therefore we chose this miR for further exploration. We tested if increased miR-9a-5p expression can affect the activity and abundance of the ENaC channel in cultured mouse cortical collecting duct (mCCD) cells. Fig. 6A and B shows the activity of native single ENaC channels in the naive mCCD cells and cells transfected with scrambled miR control oligonucleotide or miR-9a-5p mimic. miR-9a-5p transfection resulted in a significant decrease in total ENaC open probability (NP_o) and the number of the channels (N), however, did not affect single channel open probability (P_o) (Fig. 6C-E), which allows us to conclude that it resulted in a decrease in ENaC expression in the cell membrane. Furthermore, we interrogated the effect of miR9a-5p over expression in the mCCD cell model on total ENaC subunit protein expression, and found that increased levels of this miR resulted in modest, but significant decreases in both β- and γ-ENaC subunits (Fig. 5E).

4. Discussion

Over the years there have been significant advances in our understanding of the RAS and its role in PKD. There is evidence of RAS activation in ADPKD [35,36]; renin, Ang II, and angiotensinogen are abundantly present in dilated tubules, and therefore may contribute to excessive tubular salt reabsorption and increased blood pressure [37,38]. RAS blockade has been shown to be beneficial for blood pressure control in ADPKD, however the effect of double RAS blockade (combining an angiotensin receptor blocker (ARB) and angiotensin converting enzyme (ACE) inhibitor therapy) was limited [39]. Recent data demonstrated that renal cystogenesis can be attenuated in ADPKD mice by an aggressive RAS blockade [40] that would target the overactive intra-renal RAS [41]. Unfortunately, as opposed to ADPKD, little is known about RAS components in ARPKD. An early case series by Kaplan et al., and another study performed in a Lewis PKD rat

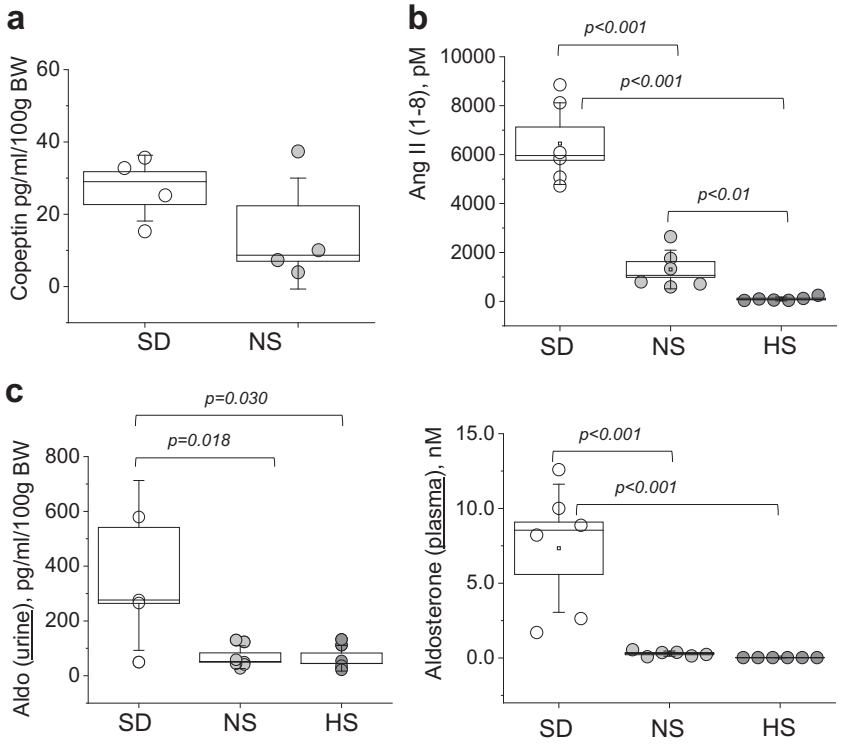

Fig. 4. Vasopressin and renin-angiotensin hormonal axes in the PCK rats after dietary treatment. (a,b) Shown are urinary copeptin (a) and circulating (plasma) Ang II (b) levels at the end of the 8 week long dietary treatment in the PCK rats fed a SD and a NS diet (for copeptin) or SD, NS and HS diets (for Ang II). Copeptin levels were undetectable in the urine of the HS diet fed PCK animals. (c) Aldosterone levels in the urine and plasma of the PCK rats fed a SD, NS and HS diets. Values were compared using a one-way ANOVA with a Tukey post-hoc test. In box plots, the box is SEM, whiskers represent SD, and line within the box shows median value.

reported a decrease in plasma renin levels [42,43]. However, a study by Loghman-Adham et al. demonstrated that expression of RAS components is elevated in ARPKD nephrectomy specimens [44]. Since those studies, the presence of the intrarenal (local) RAS has been identified, and it has been shown that this alternative RAS system is regulated separately from circulating RAS components, and is very important in renal disease states [45–47]. Dell and colleagues reported that intrarenal renin, ACE and Ang II expression were increased in the ARPKD cystic kidneys compared to age-matched Sprague Dawley rats [48]. These studies lead to a hypothesis that ACE inhibitors may be useful in the treatment of ARPKD. A recent paper by Kaimori el al. provided an intriguing and novel mechanistic explanation for cellular and phenotypic abnormalities seen in ARPKD (via NEDD4-family ligase dysfunction) [20]. In this manuscript, we examined the effects of dietary sodium on RAS in ARPKD, and uncovered a new mechanism that contributes to the detrimental consequences of a sodium-deficient diet in this disease setting.

Dietary sodium restriction is known to enhance RAS activity; however, some studies indicate that moderation of salt intake may potentiate renal and cardiovascular protective effects of ARBs and ACE inhibitors [8,49–51]. Therefore, sodium restriction is recommended together with ACE inhibitors to enhance the renoprotective benefit. However, other studies report that ACE inhibition may have adverse renal effects during dietary sodium restriction, and there is dissociation between the anti-proteinuric effect of ACE inhibition and lack of protection against structural renal abnormalities [52,53]. To date there is no evidence-based reason to support salt intake restrictions for ARPKD patients apart from general recommendations for all CKD patients. Intrarenal RAS was shown to be activated in PKD [41], and RAS suppression may attenuate renal cystogenesis [54]. It is well-known that salt restriction results in RAS activation. On the one hand, moderation of sodium intake was reported to potentiate the beneficial effects of RAS inhibitors in renal diseases [8,52,55]. On the other hand, it was demonstrated that excessive sodium restriction in combination with ACE inhibitors may promote tubulointerstitial damage. Our study showed that a sodium-deficient diet results in further activation of RAS in ARPKD and promotes cyst growth. ARPKD rats fed a SD diet presented with significant renal hypertrophy and increased cystic index (overall, and cortical) compared to NS and HS fed rats. Additionally, we showed that circulating RAS levels were significantly enhanced in salt-restricted animals, and this might have contributed to the observed cyst expansion in the cortical area. Sodium restriction is a potent stimulator of the RAS in the normal physiological conditions [56]. In Sprague Dawley rats, which share a genetic background with PCK rats and can be considered a control strain, salt-depleted diet also increases plasma renin activity, angiotensin-II level and aldosterone production [57–60]. The present study indicates that PCK rats have similar response to low dietary sodium.

In order to identify the mechanism responsible for the cortical cyst growth, we investigated the role of sodium transport in the cortical collecting ducts. Despite extensive research efforts, our knowledge about the ion transport properties of the cells that comprise the cysts remains limited [61]. Evidence from experimental models suggests that transepithelial sodium and fluid secretion may contribute to cyst growth [62,63]. However, there is no consensus on whether sodium secretion is increased or decreased in cystic cells, and what the distribution pattern of sodium channels and transporters in these cells is [20,64,65].

ENaC, a major determinant of final sodium reabsorption in the distal nephron, is known to be activated by RAS components such as Ang II and aldosterone [66]; aldosterone is known to be a primary ENaC activator [67,68]. Therefore, it was tempting to test ENaC as a target that might be involved in ARPKD cyst growth; however, involvement of ENaC in the development of PKD remains a controversial question. Two studies performed on monolayers of ARPKD mutant vs. rescued *orpk* PC monolayers revealed higher ENaC-mediated current in mutant

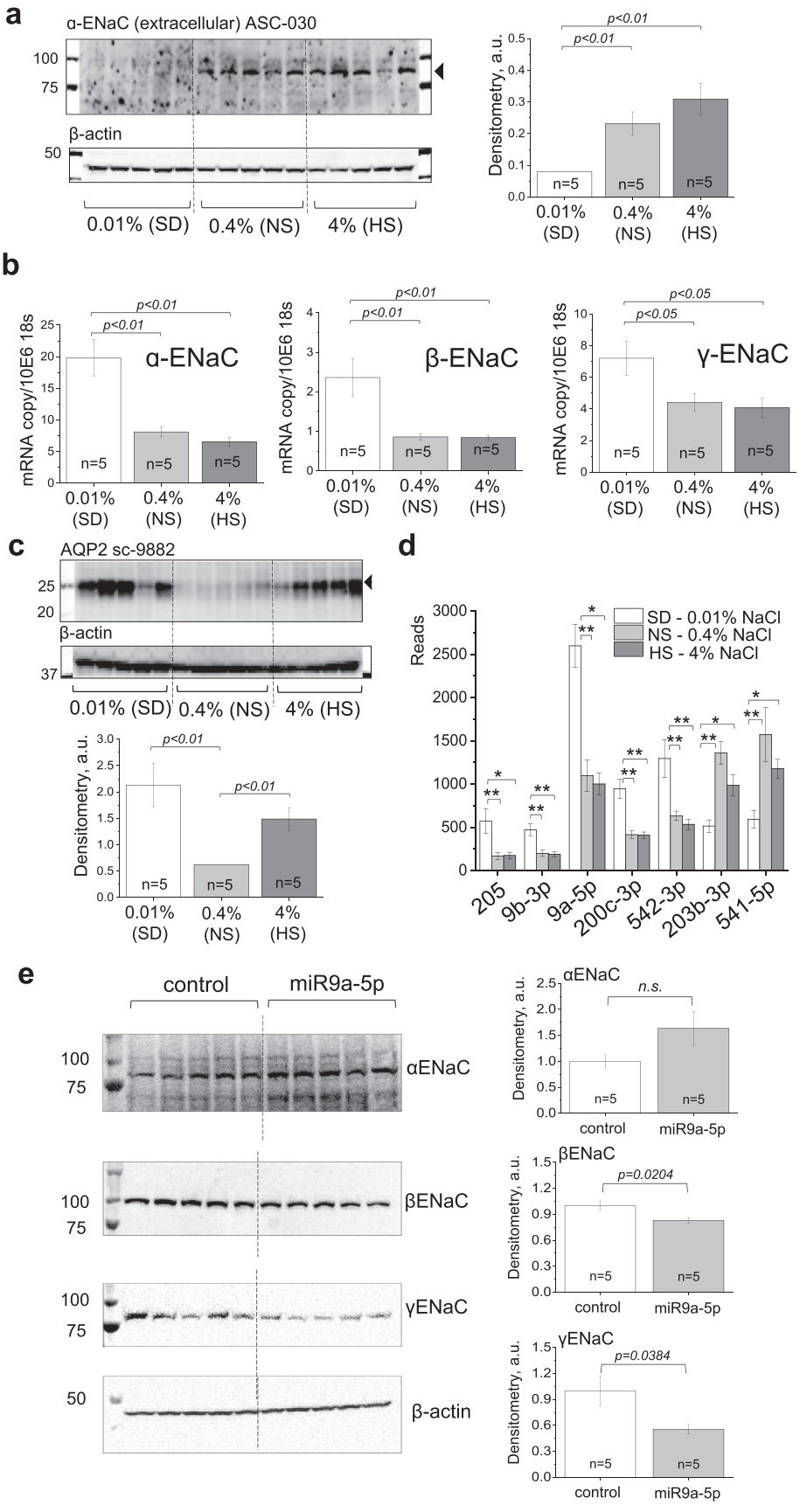

cells [69]. Recently, tubules of PCK rats were shown to have higher expression of ENaC compared to control Crj:CD/SD strain, and the authors also found elevated apical abundance of ENaC and amiloride-sensitive transepithelial current in cultured PCK CD cells [20]. In accordance with these data, analyses of ARPKD nephrectomy specimens collected at the time of renal transplantation show low sodium level in cystic

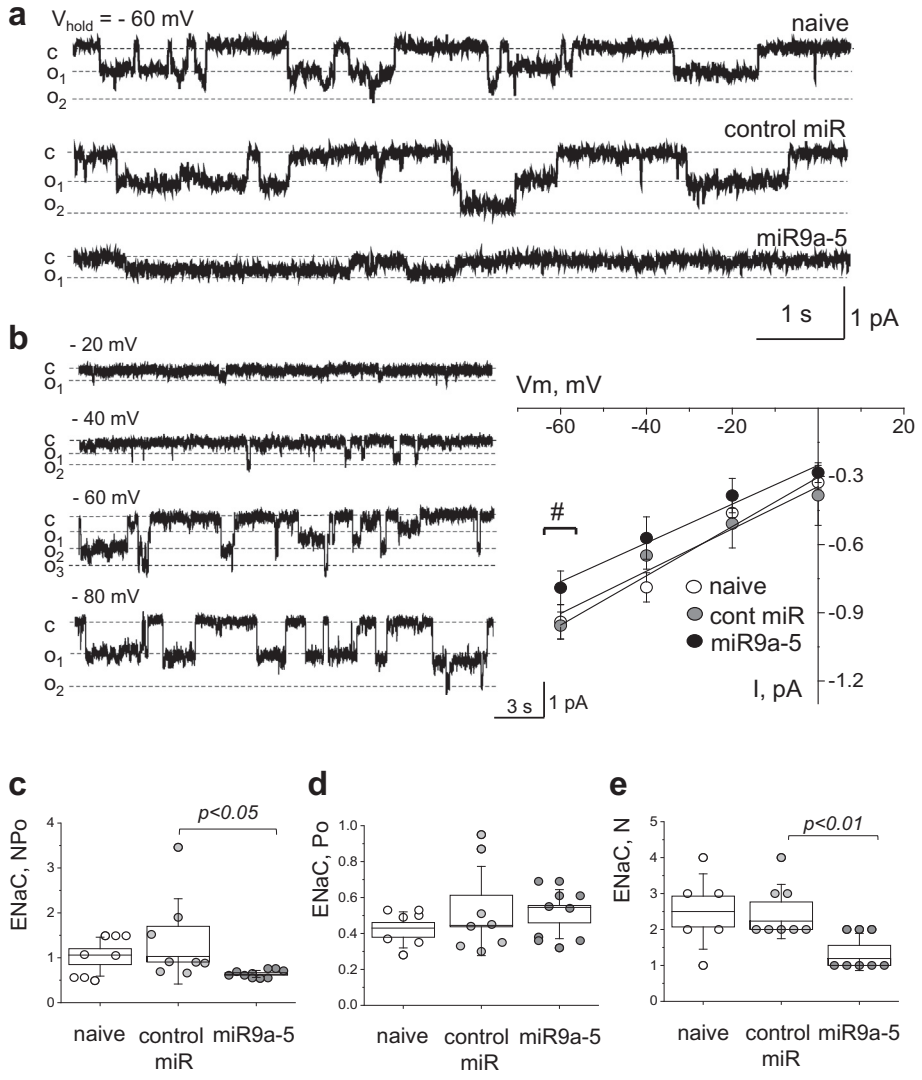

Fig. 6. ENaC activity is altered in the miR-9a-5 overexpressed experimental group. (a) Representative gap-free current traces from cell-attached patches made on mCCD cells of naïve, untransfected cells (upper), control (cont) miR with a non-specific targeting sequence (middle) and miR-9a-5 (lower) group. The closed *(c)* and open *(o)* states are denoted with dashed lines. Currents were recorded at the membrane voltage of −60 mV. # denotes $p < .05$ between control group and miR9a-5 group. (b) Current-voltage relationship and representative examples of ENaC single-channel current at different membrane potentials made on mCCD cells of miR group. (c,d,e) Summary graphs of NP_o (c), P_o (d), and N (e) for ENaC activity in naïve (white), control miR (dark grey) and miR-9a-5 (black) groups. $^*P < .05$, $^{**}P < .01$, *ns* – not statistically significant, miR9a-5 versus control-miR group by ANOVA**.** Values were compared using a one-way ANOVA with a Tukey post-hoc test. In box plots, the box is SEM, whiskers represent SD, and line within the box shows median value.

fluid [70]. Earlier, Rohatgi and colleagues employed in vivo studies in immortalized human ARPKD and age-matched collecting tubule (HFCT) cells grown on permeable supports and found that ARPKD cells absorbed Na^+ at a rate approximately 50% greater than that of HFCT [71]. Also the authors found that in two kidneys harvested from 1-month old infants with ARPKD, α-ENaC expression was approximately 2 times greater than age-matched control kidneys [71]. On the other hand, Veizis et al. have shown that amiloride sensitive Na^+ absorption is decreased in CD cells from the non-orthologous BPK mouse model of ARPKD. These and other authors have proposed that impaired sodium reabsorption, particularly, resulting from aberrant EGF signaling) plays a role in cystogenesis [72–75]. Our earlier studies in PCK rats indicate that large mature cysts exhibit low ENaC activity and abundance. Therefore, observations of ENaC function in ARPKD significantly vary in different experimental models and type of tissues. Benzamil treatment, for instance, decreased cyst size in MDCK 3D culture [76] but aggravated cyst growth in vivo.

Despite our initial expectation that ENaC expression would be increased in the salt-restricted animals due to RAS activation, we observed a complete loss of αENaC protein in the cortical tissue of the SD-diet fed rats (Fig. 5). Potentially, cystic tissue may be unresponsive to elevated aldosterone due to the loss of the mineralocorticoid receptor

Fig. 5. ENaC protein and mRNA expression in PCK rats fed diets with varying sodium content. (a) Western blotting showing expression levels of α-ENaC in the renal cortex of the PCK rats fed a SD, NS and HS diets, and a summary graph with densitometry values (normalized to β-actin expression for the same samples). Each lane on the blot is one animal. (b) mRNA expression for α-, β-, and γ-ENaC in the renal cortex of the PCK rats fed a SD, NS and HS diets. (c) Western blotting showing expression levels of AQP2 in the renal cortex of the PCK rats fed a SD, NS and HS diets, and a summary graph with densitometry values (normalized to β-actin expression for the same samples). (d) miRNAs found to be differentially expressed ($p < .05$) in the cortical tissues of the PCK rats fed a SD, NS and HS diets. *, $p < .05$, **$p < .01$. (e) Western blots demonstrating total ENaC subunit expression in cultured mCCD cells transfected with a control scrambled miR sequence or miR9a-5p, with summary densitometry graphs (normalized to β-Actin and relative to control mCCD expression). Both β- and γ-ENaC are significantly decreased in mCCD cells over expressing miR9a-5p. * $p < .05$. Values in (b) and (c) were compared using a one-way ANOVA with a Tukey post-hoc test. For (d), differential expression was determined by DESeq2 method [34]. False discovery rate within statistical analysis was controlled for using the Benjamini-Hochberg method, p value cutoff was 0.05. Graphs with whiskers show mean value in each group and SEM. In (e), following a Shapiro-Wilk normality test, control and experimental values were compared using an unpaired student t-test.

(MR) in the cystic cells that undergo epithelial-to-mesenchymal transition. Subjects with hypertension and PKD were shown to have higher plasma renin activity and plasma aldosterone concentration than patients with essential hypertension, which indicates that RAS is stimulated significantly more [77]. The HALT-PKD trial [78] revealed that urine aldosterone levels declined similarly in study participants taking both lower and higher doses of RAS inhibitors Lisinopril and Telmisartan. In Lewis PKD rat, MR antagonism with spironolactone has proven an effective means to control hypertension, but had no effect on cyst growth or kidney morphology [79]. There are clinical reports suggesting that ADPKD and primary aldosteronism are connected and there might be a role for aldosterone excess and the resultant hypokalemia in promoting cyst growth [80]. However, the question of whether antagonism of MR should be used effectively in combination with RAS antagonism to treat PKD, remains open [81].

We demonstrated that all three ENaC subunits' mRNA levels were significantly increased in the salt-restricted group. This led to a hypothesis that a miRNA might be regulating ENaC post-transcriptional expression; we found multiple differentially expressed miRNAs among the studied groups. miR-9a-5p was highly expressed in the SD-treated group, and was predicted to regulate βENaC expression through seed region complementarity with the 3'-UTR. Our cell culture studies indicate that overexpression of miR-9a-5p reduced ENaC abundance and activity in mCCD cells. Here we have identified a novel miR capable of regulating the expression of ENaC; to date, there are only a few miRNAs known to affect ENaC in various tissues and cell types. Kim et al. demonstrated that miR-263a regulates ENaC to maintain osmotic and intestinal stem cell homeostasis (in *Drosophilae* [82]). In the distal nephron of the kidney, the miRNA cluster miR-23-24-27 was demonstrated to be able to alter sodium transport via an aldosterone-dependent regulation [83]. In the alveolar epithelium microRNA-7-5p affected ENaC by targeting the mTORC2/SGK-1 signaling pathway [84]. Emerging evidence from studies on animal models and specimens obtained from PKD patients suggest that aberrant expression of many miRNAs may underlie the progression of this disease: for example, inhibiting miR-17, miR-21 or increasing levels of miR-200 and related miRNAs has been suggested to retard PKD progression [85,86]. miRNAs are a powerful tool to prevent cyst enlargement through regulation of key aspects of epithelia pathogenesis, such as proliferation and apoptosis of cyst epithelia, and regulation of PKD gene dosage. Thus, there is a potential for the use of synthetic anti-miRs and miRNA-mimics as a basis for a new therapeutic approach to PKD, and further studies are required to definitively conclude that ENaC protein is under the regulatory influence of the miR-9a-5p in the animal cyst model or in ARPKD cysts.

In conclusion, we have identified that salt restriction aggravates cyst development in a rat model of ARPKD, and this is accompanied by down-regulation of ENaC expression; we have also found a dramatic increase in miR-9a-5p expression in this setting, which is predicted to interact with βENaC subunit mRNA, although more targeted translational experiments such as 3'UTR luciferase assays are needed to determine whether the changes to ENaC expression are direct miR binding or through a secondary regulatory pathway. In cultured CCD cells we have demonstrated that miR-9a-5p affects ENaC expression and the number of the channels in the membrane; therefore, this observed reduction may contribute to cortical cyst development. Since miR-9a-5p is predicted to repress multiple mRNA targets within the same pathways, it could be regulating an entire signaling node in ARPKD; however, without additional studies this remains conjecture. Our data demonstrate that perhaps there is a need to exercise additional care when salt-restricting ARPKD patients. A relationship between the observed cystic phenotype, RAS and miRNA-mediated decrease in ENaC-mediated sodium reabsorption identified here advanced our understanding of the control of sodium balance in ARPKD, and has potential implications in other diseases associated with imbalances of sodium and water homeostasis. However, current study also should be considered cautiously since sodium-deficient diet used here cannot be easily translated to human diet.

Declaration of interests

Dr. Ilatovskaya reports grants from National Institute of Health and PKD Foundation. Dr. Pavlov and Dr. Klemens reports grants from National Institute of Health. Mr. Levchenko, Dr. Isaeva, Ms. Johnson, Dr. Liu, and Dr. Kriegel have nothing to disclose. Dr. Staruschenko reports grants from National Institute of Health, Department of Veteran Affairs, and American Heart Association during the conduct of the study; grants from National Institute of Health, Department of Veteran Affairs, American Heart Association, and American Diabetes Association outside the submitted work.

Funding

National Institute of Health grantsR35 HL135749, P01 HL116264 (AS), DK090868 via Baltimore PKD Center and R00 HL116603 (TSP), R00 DK105160 (DVI), T32 HL134643 (CAK), Department of Veteran AffairsI01 BX004024 (AS), PKD Foundation Research grant 221G18a (DVI), and American Heart Association16EIA26720006 (AS).

Author contribution

Conceptualization: DVI and AS; investigation: DVI, VL, TSP, EI, CAK, JJ; analysis: DVI, PL, AJK; writing original draft – DVI; writing, review, editing, and final approval: DVI, VL, TSP, EI, CAK, JJ, PL, AJK, AS; resources and supervision: AS.

Acknowledgements

We would like to thank Mark Paterson, Sandy Chuppa, Christine Duris, Lisa Henderson, and Camille Torres (all Medical College of Wisconsin) for technical help and analyses.

Appendix A. Supplementary data

Supplementary data to this article can be found online at https://doi.org/10.1016/j.ebiom.2019.01.006.

References

[1] Wilson PD. Polycystic kidney disease. N Engl J Med 2004;350:151–64.
[2] Guay-Woodford LM, Desmond RA. Autosomal recessive polycystic kidney disease: the clinical experience in North America. Pediatrics 2003;111:1072–80.
[3] Klein JD, Blount MA, Sands JM. Urea transport in the kidney. Compr Physiol 2011;1:699–729.
[4] Farquhar WB, Edwards DG, Jurkovitz CT, Weintraub WS. Dietary sodium and health: more than just blood pressure. J Am Coll Cardiol 2015;65:1042–50.
[5] He FJ, MacGregor GA. A comprehensive review on salt and health and current experience of worldwide salt reduction programmes. J Hum Hypertens 2009;23(6):363–84.
[6] Middleton JP, Lehrich RW. Prescriptions for dietary sodium in patients with chronic kidney disease: how will this shake out? Kidney Int 2014;86(3):457–9.
[7] DiNicolantonio JJ, Niazi AK, Sadaf R, JH OK, Lucan SC, Lavie CJ.. Dietary sodium restriction: take it with a grain of salt. Am J Med 2013;126:951–5.
[8] Lambers Heerspink HJ, Holtkamp FA, Parving HH, Navis GJ, Lewis JB, Ritz E, et al. Moderation of dietary sodium potentiates the renal and cardiovascular protective effects of angiotensin receptor blockers. Kidney Int 2012;82:330–7.
[9] O'Donnell MJ, Yusuf S, Mente A, Gao P, Mann JF, Teo K, et al. Urinary sodium and potassium excretion and risk of cardiovascular events. JAMA 2011;306:2229–38.
[10] Weimbs T, Shillingford JM, Torres J, Kruger SL, Bourgeois BC. Emerging targeted strategies for the treatment of autosomal dominant polycystic kidney disease. Clin Kidney J 2018;11:i27–38.
[11] Chapman AB, Devuyst O, Eckardt KU, Gansevoort RT, Harris T, Horie S, et al. Autosomal-dominant polycystic kidney disease (ADPKD): executive summary from a kidney disease: improving global outcomes (KDIGO) controversies conference. Kidney Int 2015;88:17–27.
[12] Tran WC, Huynh D, Chan T, Chesla CA, Park M. Understanding barriers to medication, dietary, and lifestyle treatments prescribed in polycystic kidney disease. BMC Nephrol 2017;18:214.
[13] Xue C, Zhou CC, Wu M, Mei CL. The clinical manifestation and management of autosomal dominant polycystic kidney disease in China. Kidney Dis 2016;2:111–9.
[14] Harris T, Sandford R, de Coninck B, Devuyst O, Drenth JPH, Ecder T, et al. European ADPKD Forum multidisciplinary position statement on autosomal dominant

polycystic kidney disease care: European ADPKD forum and multispecialist roundtable participants. Nephrol Dial Transplant 2017. https://doi.org/10.1093/ndt/gfx327.
[15] Potts JW, Mousa SA. Recent advances in management of autosomal-dominant polycystic kidney disease. Am J Health Syst Pharm 2017;74:1959–68.
[16] Torres VE, Abebe KZ, Schrier RW, Perrone RD, Chapman AB, Yu AS, et al. Dietary salt restriction is beneficial to the management of autosomal dominant polycystic kidney disease. Kidney Int 2017;91:493–500.
[17] Taylor JM, Hamilton-Reeves JM, Sullivan DK, Gibson CA, Creed C, Carlson SE, et al. Diet and polycystic kidney disease: a pilot intervention study. Clin Nutr 2017;36:458–66.
[18] Torres VE, Grantham JJ, Chapman AB, Mrug M, Bae KT, King Jr BF, et al. Potentially modifiable factors affecting the progression of autosomal dominant polycystic kidney disease. Clin J Am Soc Nephrol 2011;6:640–7.
[19] Canessa CM, Schild L, Buell G, Thorens B, Gautschi I, Horisberger JD, et al. Amiloride-sensitive epithelial Na^+ channel is made of three homologous subunits. Nature 1994;367:463–7.
[20] Kaimori JY, Lin CC, Outeda P, Garcia-Gonzalez MA, Menezes LF, Hartung EA, et al. NEDD4-family E3 ligase dysfunction due to PKHD1/Pkhd1 defects suggests a mechanistic model for ARPKD pathobiology. Sci Rep 2017;7:7733.
[21] Olteanu D, Yoder BK, Liu W, Croyle MJ, Welty EA, Rosborough K, et al. Heightened epithelial Na+ channel-mediated Na+ absorption in a murine polycystic kidney disease model epithelium lacking apical monocilia. Am J Physiol Cell Physiol 2006;290:C952–63.
[22] Gray MA. Primary cilia and regulation of renal Na^+ transport. Focus on "heightened epithelial Na^+ channel-mediated Na^+ absorption in a murine polycystic kidney disease model epithelium lacking apical monocilia". Am J Physiol Cell Physiol 2006;290:C947–9.
[23] Pavlov TS, Levchenko V, Ilatovskaya DV, Palygin O, Staruschenko A. Impaired epithelial Na+ channel activity contributes to cystogenesis and development of autosomal recessive polycystic kidney disease in PCK rats. Pediatr Res 2015;77:64–9.
[24] Katsuyama M, Masuyama T, Komura I, Hibino T, Takahashi H. Characterization of a novel polycystic kidney rat model with accompanying polycystic liver. Exp Anim 2000;49:51–5.
[25] Lager DJ, Qian Q, Bengal RJ, Ishibashi M, Torres VE. The pck rat: a new model that resembles human autosomal dominant polycystic kidney and liver disease. Kidney Int 2001;59:126–36.
[26] Nagao S, Kugita M, Yoshihara D, Yamaguchi T. Animal models for human polycystic kidney disease. Exp Anim 2012;61:477–88.
[27] Ilatovskaya DV, Blass G, Palygin O, Levchenko V, Pavlov TS, Grzybowski MN, et al. A NOX4/TRPC6 pathway in podocyte calcium regulation and renal damage in diabetic kidney disease. J Am Soc Nephrol 2018;29(7):1917–27.
[28] Rieg T. A High-throughput method for measurement of glomerular filtration rate in conscious mice. J Vis Exp 2013;75:e50330.
[29] Palygin O, Levchenko V, Ilatovskaya DV, Pavlov TS, Pochynyuk OM, Jacob HJ, et al. Essential role of Kir5.1 channels in renal salt handling and blood pressure control. JCI Insight 2017;2(18) (pii: 92331).
[30] Pavlov TS, Chahdi A, Ilatovskaya DV, Levchenko V, Vandewalle A, Pochynyuk O, et al. Endothelin-1 inhibits the epithelial Na^+ channel through betaPix/14-3-3/Nedd4-2. J Am Soc Nephrol 2010;21:833–43.
[31] Gaeggeler HP, Gonzalez-Rodriguez E, Jaeger NF, Loffing-Cueni D, Norregaard R, Loffing J, et al. Mineralocorticoid versus glucocorticoid receptor occupancy mediating aldosterone-stimulated sodium transport in a novel renal cell line. J Am Soc Nephrol 2005;16:878–91.
[32] Kriegel AJ, Liu Y, Cohen B, Usa K, Liu Y, Liang M. MiR-382 targeting of kallikrein 5 contributes to renal inner medullary interstitial fibrosis. Physiol Genomics 2012;44(4):259–67.
[33] Kriegel AJ, Liu Y, Liu P, Baker MA, Hodges MR, Hua X, et al. Characteristics of microRNAs enriched in specific cell types and primary tissue types in solid organs. Physiol Genomics 2013;45:1144–56.
[34] Love MI, Huber W, Anders S. Moderated estimation of fold change and dispersion for RNA-seq data with DESeq2. Genome Biol 2014;15(12):550.
[35] Kocyigit I, Yilmaz MI, Unal A, Ozturk F, Eroglu E, Yazici C, et al. A link between the intrarenal renin angiotensin system and hypertension in autosomal dominant polycystic kidney disease. Am J Nephrol 2013;38(3):218–25.
[36] Saigusa T, Bell PD. Molecular pathways and therapies in autosomal-dominant polycystic kidney disease. Physiology (Bethesda) 2015;30(3):195–207.
[37] Graham PC, Lindop GB. The anatomy of the renin-secreting cell in adult polycystic kidney disease. Kidney Int 1988;33(6):1084–90.
[38] Torres VE, Donovan KA, Scicli G, Holley KE, Thibodeau SN, Carretero OA, et al. Synthesis of renin by tubulocystic epithelium in autosomal-dominant polycystic kidney disease. Kidney Int 1992;42(2):364–73.
[39] Torres VE, Abebe KZ, Chapman AB, Schrier RW, Braun WE, Steinman TI, et al. Angiotensin blockade in late autosomal dominant polycystic kidney disease. N Engl J Med 2014;371(24):2267–76.
[40] Fitzgibbon WR, Dang Y, Bunni MA, Baicu CF, Zile MR, Mullick AE, et al. Attenuation of accelerated renal cystogenesis in Pkd1 mice by renin angiotensin system blockade. Am J Physiol Renal Physiol 2018;314(2) (F210-F218).
[41] Saigusa T, Dang Y, Bunni MA, Amria MY, Steele SL, Fitzgibbon WR, et al. Activation of the intrarenal renin-angiotensin-system in murine polycystic kidney disease. Physiol Rep 2015;3(5) (pii: e12405).
[42] Kaplan BS, Fay J, Shah V, Dillon MJ, Barratt TM. Autosomal recessive polycystic kidney disease. Pediatr Nephrol 1989;3(1):43–9.
[43] Phillips JK, Hopwood D, Loxley RA, Ghatora K, Coombes JD, Tan YS, et al. Temporal relationship between renal cyst development, hypertension and cardiac hypertrophy in a new rat model of autosomal recessive polycystic kidney disease. Kidney Blood Press Res 2007;30(3):129–44.
[44] Loghman-Adham M, Soto CE, Inagami T, Sotelo-Avila C. Expression of components of the renin-angiotensin system in autosomal recessive polycystic kidney disease. J Histochem Cytochem 2005;53(8):979–88.
[45] Carey RM. The intrarenal renin-angiotensin system in hypertension. Adv Chronic Kidney Dis 2015;22(3):204–10.
[46] Culver S, Li C, Siragy HM. Intrarenal angiotensin-converting enzyme: the old and the new. Curr Hypertens Rep 2017;19(10):80.
[47] Yang T, Xu C. Physiology and pathophysiology of the intrarenal renin-angiotensin system: an update. J Am Soc Nephrol 2017;28(4):1040–9.
[48] Goto M, Hoxha N, Osman R, Dell KM. The renin-angiotensin system and hypertension in autosomal recessive polycystic kidney disease. Pediatr Nephrol 2010;25(12):2449–57.
[49] Wapstra FH, Van Goor H, Navis G, De Jong PE, De Zeeuw D. Antiproteinuric effect predicts renal protection by angiotensin-converting enzyme inhibition in rats with established adriamycin nephrosis. Clin Sci 1996;90(5):393–401.
[50] Wing LM, Arnolda LF, Harvey PJ, Upton J, Molloy D, Gabb GM, et al. Low-dose diuretic and/or dietary sodium restriction when blood pressure is resistant to ACE inhibitor. Blood Press 1998;7(5–6):299–307.
[51] Teravainen TL, Mervaala EM, Laakso J, Paakkari I, Vapaatalo H, Karppanen H. Influence of age on cardiovascular effects of increased dietary sodium and angiotensin-converting enzyme inhibition in normotensive Wistar rats. J Pharm Pharmacol 1997;49(9):912–8.
[52] Hamming I, Navis G, Kocks MJ, van Goor H. ACE inhibition has adverse renal effects during dietary sodium restriction in proteinuric and healthy rats. J Pathol 2006;209(1):129–39.
[53] Smit-van Oosten A, Navis G, Stegeman CA, Joles JA, Klok PA, Kuipers F, et al. Chronic blockade of angiotensin II action prevents glomerulosclerosis, but induces graft vasculopathy in experimental kidney transplantation. J Pathol 2001;194(1):122–9.
[54] Saigusa T, Dang Y, Mullick AE, Yeh ST, Zile MR, Baicu CF, et al. Suppressing angiotensinogen synthesis attenuates kidney cyst formation in a Pkd1 mouse model. FASEB J 2016;30(1):370–9.
[55] Humalda JK, Navis G. Dietary sodium restriction: a neglected therapeutic opportunity in chronic kidney disease. Curr Opin Nephrol Hypertens 2014;23(6):533–40.
[56] Williams JS, Williams GH. 50th anniversary of aldosterone. J Clin Endocrinol Metab 2003;88(6):2364–72.
[57] Palmore WP, Mulrow PJ. Control of aldosterone secretion by the pituitary gland. Science 1967;158:1482–4.
[58] Gomez-Sanchez C, Holland OB, Higgins JR, Kem DC, Kaplan NM. Circadian rhythms of serum renin activity and serum corticosterone, prolactin, and aldosterone concentrations in the male rat on normal and low-sodium diets. Endocrinology 1976;99:567–72.
[59] Höcherl K, Kammerl MC, Schumacher K, Endemann D, Grobecker HF, Kurtz A. Role of prostanoids in regulation of the renin-angiotensin-aldosterone system by salt intake. Am J Physiol Renal Physiol 2002;283 (F294-F301).
[60] Adler GK, Chen R, Menachery AI, Braley LM, Williams GH. Sodium restriction increases aldosterone biosynthesis by increasing late pathway, but not early pathway, messenger ribonucleic acid levels and enzyme activity in normotensive rats. Endocrinology 1993;133(5):2235–40.
[61] Sullivan LP, Wallace DP, Grantham JJ. Epithelial transport in polycystic kidney disease. Physiol Rev 1998;78(4):1165–91.
[62] Veizis EI, Carlin CR, Cotton CU. Decreased amiloride-sensitive Na+ absorption in collecting duct principal cells isolated from BPK ARPKD mice. Am J Physiol Renal Physiol 2004;286(2) F244-F254.
[63] Wildman SS, Kang ES, King BF. ENaC, renal sodium excretion and extracellular ATP. Purinergic Signal 2009;5(4):481–9.
[64] Zheleznova NN, Wilson PD, Staruschenko A. Epidermal growth factor-mediated proliferation and sodium transport in normal and PKD epithelial cells. Biochim Biophys Acta 2011;1812(10):1301–13.
[65] Rodriguez D, Kapoor S, Edenhofer I, Segerer S, Riwanto M, Kipar A, et al. Inhibition of sodium-glucose cotransporter 2 with dapagliflozin in Han: SPRD rats with polycystic kidney disease. Kidney Blood Press Res 2015;40(6):638–47.
[66] Zaika O, Mamenko M, Staruschenko A, Pochynyuk O. Direct activation of ENaC by angiotensin II: recent advances and new insights. Curr Hypertens Rep 2013;15(1):17–24.
[67] Hummler E. Epithelial sodium channel, salt intake, and hypertension. Curr Hypertens Rep 2003;5(1):11–8.
[68] Eaton DC, Malik B, Saxena NC, Al-Khalili OK, Yue G. Mechanisms of aldosterone's action on epithelial Na^+ transport. J Membr Biol 2001;184(3):313–9.
[69] Saigusa T, Reichert R, Guare J, Siroky BJ, Gooz M, Steele S, et al. Collecting duct cells that lack normal cilia have mislocalized vasopressin-2 receptors. Am J Physiol Renal Physiol 2012;302(7) (F801-F8).
[70] Rohatgi R, Zavilowitz B, Vergara M, Woda C, Kim P, Satlin LM. Cyst fluid composition in human autosomal recessive polycystic kidney disease. Pediatr Nephrol 2005;20(4):552–3.
[71] Rohatgi R, Greenberg A, Burrow CR, Wilson PD, Satlin LM. Na transport in autosomal recessive polycystic kidney disease (ARPKD) cyst lining epithelial cells. J Am Soc Nephrol 2003;14(4):827–36.
[72] Veizis IE, Cotton CU. Abnormal EGF-dependent regulation of sodium absorption in ARPKD collecting duct cells. Am J Physiol Renal Physiol 2005;288(3) (F474-F82).
[73] Falin R, Veizis IE, Cotton CU. A role for ERK1/2 in EGF- and ATP-dependent regulation of amiloride-sensitive sodium absorption. Am J Physiol Cell Physiol 2005;288(5)(C1003-C1011).
[74] Wilson PD. Apico-basal polarity in polycystic kidney disease epithelia. Biochim Biophys Acta 2011;1812(10):1239–48.
[75] Wilson PD. A plethora of epidermal growth factor-like proteins in polycystic kidneys. Kidney Int 2004;65(6):2441–2.

[76] Grantham JJ, Uchic M, Cragoe EJ, Kornhaus J, Grantham JA, Donoso V, et al. Chemical modification of cell proliferation and fluid secretion in renal cysts. Kidney Int 1989; 35(6):1379–89.
[77] Chapman AB, Johnson A, Gabow PA, Schrier RW. The renin-angiotensin-aldosterone system and autosomal dominant polycystic kidney disease. N Engl J Med 1990;323 (16):1091–6.
[78] Brosnahan GM, Abebe KZ, Moore CG, Bae KT, Braun WE, Chapman AB, et al. Determinants of progression in early autosomal dominant polycystic kidney disease: is it blood pressure or renin-angiotensin-aldosterone-system blockade? Curr Hypertens Rev 2018;14:39–47.
[79] Jeewandara TM, Ameer OZ, Boyd R, Wyse BF, Underwood CF, Phillips JK. Protective cardiorenal effects of spironolactone in a rodent model of polycystic kidney disease. Clin Exp Pharmacol Physiol 2015;42(4):353–60.
[80] Peixoto AJ. A young patient with a family history of hypertension. Clin J Am Soc Nephrol 2014;9(12):2164–72.
[81] Hian CK, Lee CL, Thomas W. Renin-angiotensin-aldosterone system antagonism and polycystic kidney disease progression. Nephron 2016;134(2):59–63.
[82] Kim K, Hung RJ, Perrimon N. miR-263a regulates ENaC to maintain osmotic and intestinal stem cell homeostasis in Drosophila. Dev Cell 2017;40(1):23–36.
[83] Liu X, Edinger RS, Klemens CA, Phua YL, Bodnar AJ, LaFramboise WA, et al. A microRNA cluster miR-23-24-27 is upregulated by aldosterone in the distal kidney nephron where it alters sodium transport. J Cell Physiol 2017;232(6):1306–17.
[84] Qin K, Zhong X, Wang D. MicroRNA-7-5p regulates human alveolar epithelial sodium channels by targeting the mTORC2/SGK-1 signaling pathway. Exp Lung Res 2016;42(5):237–44.
[85] Yheskel M, Patel V. Therapeutic microRNAs in polycystic kidney disease. Curr Opin Nephrol Hypertens 2017;26(4):282–9.
[86] Hajarnis S, Lakhia R, Patel V. MicroRNAs and polycystic kidney disease. In: Li X, editor. Polycystic Kidney Disease; 2015.